Effects of Inhibitory Synaptic Current Parameters on Thalamocortical Oscillations

Scott Cole
Neurosciences Graduate Program
University of California, San Diego
La Jolla, CA 92093-0634
scott.cole0@gmail.com

Richard Gao
Department of Cognitive Science
UCSD
La Jolla, CA 92093-0515
rigao@ucsd.edu

Abstract

We explore the role of specific GABAergic current conductance and decay time in specific inhibitory synapses in driving macroscopic cortical oscillations based on two computational neuron models. Simulations using a previously established thalamocortical network model demonstrate that: 1) oscillation frequency changes due to increased inhibitory conductance are dependent on post-synaptic neuron type, 2) changes in inhibitory current decay time have no effect on oscillation frequency, and 3) large changes in inhibitory conductance can produce dynamic changes in the network behavior that is uncaptured by peak oscillation frequency. These results warrant careful treatment of different types of GABA recipients in computational models, and motivate further investigation in the effects of substances which promote GABAergic activity, such as propofol.

1 Introduction

Oscillatory electrical activities are observed in brains and brain regions [1] and have been instrumental in the analysis of electrophysiological data recorded with macroelectrodes, such as electroencephalography (EEG) [2]. Although these brain rhythms have been studied extensively in the past century, their mechanisms of origin and purpose have largely remained mysteries. Recently, there have been several models of neural networks created to replicate the emergence of brain rhythms of different varieties, characterized by the frequency band with the highest power [1,3]. In particular, sub-gamma rhythms (<30Hz) observed in EEG have been explained as the result of a thalamocortical loop that evokes periodic responses in cortical pyramidal neurons [4], which are oriented suitably to contribute to the EEG recordings [5].

Ching, et al. previously published the simulated response of a thalamocortical model to the anesthetic drug, propofol [6]. They modeled propofol as a systemic increase in the inhibitory $GABA_A$ conductance and time constant. A decrease in oscillation frequency from low gamma (~40Hz) to alpha rhythms (~10Hz) was observed in the modeled cortical pyramidal cells during simulated anesthesia. This result matched experimental observations of subjects' EEG recordings when losing consciousness after receiving doses of propofol. In this report, we independently manipulated the synaptic current projections between different neuron classes in a thalamocortical model to identify the effects of each projection on the system's overall response.

2 Models and Methods

The thalamocortical loop was modeled using the Brian 2.0 package in Python [7]. Neurons

were modeled using either the adaptive-exponential integrate-and-fire (aeIF) model (eq. 1) [8,9] or Izhikevich neurons (eq. 2) [10]. The model parameters of the aeIF neurons (a,b) were defined for each cell type in the thalamocortical circuit as by Destexhe [8]. The parameters for the Izhikevich neurons (a,b,c,d) were provided in [10] for the thalamic and cortical cells in the network.

Neuron groups and synapses were organized as illustrated in Figure 1. Four classes of neurons were modeled: pyramidal cortical neurons (PY), fast-spiking cortical interneurons (FS), thalamocortical relay neurons (TC), and thalamic reticular neurons (RE). Excitatory neurons (PY and TC) made synapses onto all other neuron groups while inhibitory neurons (FS and RE) projected only to both neuron groups within their own layer.

The connection probability between neurons was 20%, except for connections from RE which had an 80% probability of occurring. Excitatory and inhibitory synaptic currents maximal conductances were 30nS at default for aeIF model, and 30μS for Izhikevich model, due to differences in intrinsic model parameters. The reversal potential for excitatory (AMPA) synaptic current was 0mV and for inhibitory (GABA) synaptic current was -80mV. The time constant for AMPA-mediated synaptic current was 5ms, and for GABA-mediated synaptic current was 10ms at default. Network activity was initiated at the start of the simulation by random excitatory input into the PY population for the first 50ms. After this time, network activity was self-sustained.

For the aeIF model, parameters were adopted from the thalamocortical model by Destexhe [8], and adjustments were made in network size and connectivity to speed up the simulation runtime. Specifically, a total of 220 neurons were simulated in the circuit for 10 seconds: 160 PY, 40 FS, 10 TC, and 10 RE.

$$C\frac{dv}{dt} = -g_L(v - E_L) + g_L\Delta_T \exp\left(\frac{v - V_T}{\Delta_T}\right) - g_{AMPA}(v - E_{AMPA}) - g_{GABA}(v - E_{GABA}) - w \quad (1)$$

$$\tau_w \frac{dw}{dt} = a(v - E_L) - w$$

$$reset: if\ v > 0mV : v \to E_L, w \to w + b$$

The Izhikevich model used similar configurations, but scaled due to intrinsic differences in the model, specifically constants in the voltage differential equation.

$$\frac{dv}{dt} = 0.04v^2 + 5v + 140 - u + I_{ext} \quad (2)$$

$$\frac{du}{dt} = a(bv - u)$$

$$reset: if\ v > 30, v = c, u = u + d$$

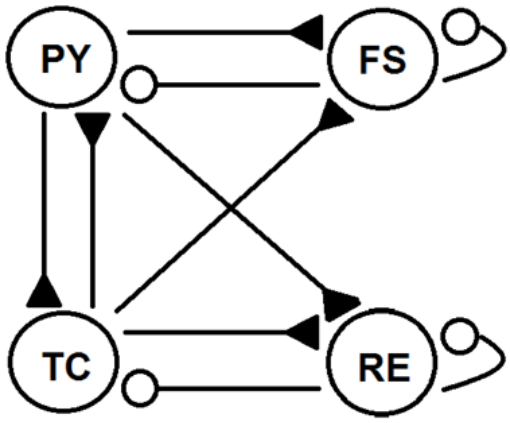

Figure 1. Schematic of network connections. Filled triangles represent excitatory synapses, and open circles indicate inhibitory synapses. The cortex (top half) is modeled with excitatory pyramidal (PY) cells and fast-spiking interneurons (FS). The thalamus is modeled by

excitatory thalamocortical cells (TC) and inhibitory thalamic reticular cells (RE). The inhibitory cells in both layers (FS and RE) inhibit the excitatory neuron group in their layer as well as themselves. The excitatory cells send projections to all other neuron groups.

EEG signals were estimated from the simulated population by convolving the pyramidal spike train with a truncated exponential function. The power spectrum was calculated by taking the fast-Fourier transform of the EEG signal. Peaks of the power spectrum were identified by smoothing the spectrum with a rectangular window (10Hz width) and defining the oscillatory frequency as the frequency component with the highest power.

In the experiments below, we varied the inhibitory synaptic current conductance (g_{GABA}) separately for each class of projections (e.g. RE to TC). The inhibitory synaptic time constant was also varied in the same manner.

3 Results

3.1 Oscillations in a thalamic circuit

In order to observe how synchrony arises in the thalamus, a small circuit of 2 TC and 2 RE cells was modeled in the absence of a cortex. The TC cells and RE cells were reciprocally connected, as were the two RE cells to each other. These neurons possess relatively high values of the 'a' parameter in the aeIF model, meaning that a hyperpolarization leads to an excitatory adaptive current, which allows for the occurrence of rebound spikes. The result, shown in Figure 2, was rhythmic spiking of the network with a period of approximately 50ms, meaning a 20Hz oscillation. The ability of the thalamic circuit to generate periodic action potentials means that it can entrain the cortical pyramidal cells in an oscillation through the TC-PY projection. The parameters of the neurons in the cortical layer and the interconnections in the circuit determine the dynamics of the system, leading to cortical oscillations of different frequencies. These oscillations that arise in the cortical pyramidal cells are observed in the following models.

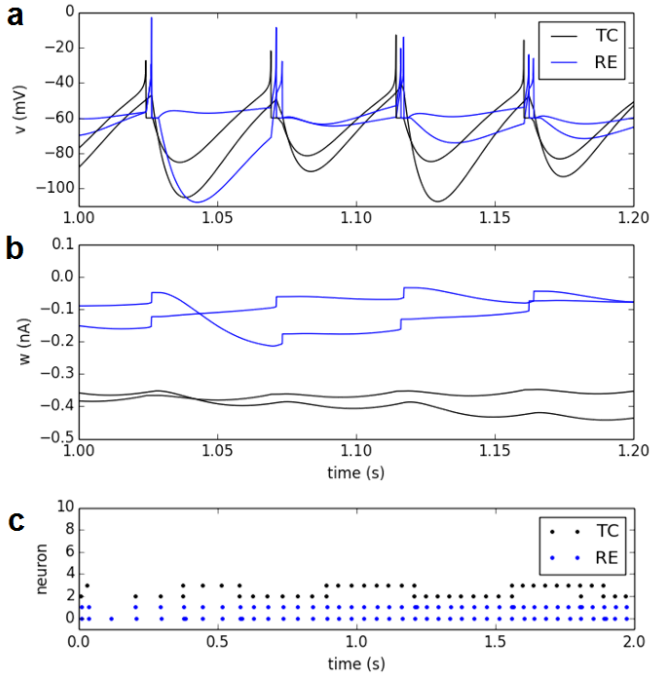

Figure 2. Two thalamocortical relay (TC) and two thalamic reticular (RE) cells interconnected produce a 20Hz oscillation. (a) Regular firing is observed in the voltage trace of both RE and TC cells. (b) The adaptive variable (w) in the aeIF model oscillates for both neurons, with the TC cells having a more negative adaptive current. (c) The raster plot of the 4-neuron network

illustrates only 1 TC cell and both RE cells typically fire in each period.

3.2 Inhibitory synaptic conductance effect on oscillatory frequency

Each of the inhibitory synaptic connections in Figure 1 was manipulated in order to modulate its effect on the model's dynamics. First, the synaptic conductance was varied between 0nS and 60nS in increments of 10nS. In Figure 3, the conductance of the RE-RE synapse was modified, and an increase in inhibitory conductance yielded a slower oscillation. However, when the RE-TC conductance was increased, as shown in Figure 4, the opposite trend was seen. An increase in RE-TC conductance from 30nS to 50nS increased the oscillation frequency by approximately 50% from a peak at 30Hz to 45Hz.

The trends for each inhibitory projection are summarized in Figure 5. In the case in which the inhibitory synaptic conductance was strengthened between two inhibitory neurons, the oscillatory frequency decreased slightly. A higher inhibitory conductance elicits a stronger inhibitory postsynaptic potential (IPSP) in the target inhibitory neuron. Therefore, that inhibitory neuron requires more excitatory current and time to reach the spike threshold, which could serve as the mechanism for a slower oscillation.

In contrast, a significantly faster oscillation is produced when the inhibitory synaptic conductance is increased to an excitatory target neuron. One possible explanation for this result is based on a shorter time window for an action potential in the excitatory cells as they experience greater inhibition. Therefore, the excitatory cells elicit EPSPs in the inhibitory cells at greater synchrony, with a high probability of eliciting a spike. This trend was also seen when all inhibitory synaptic conductances were changed together, which is in direct contrast to the results of Ching et al. [6].

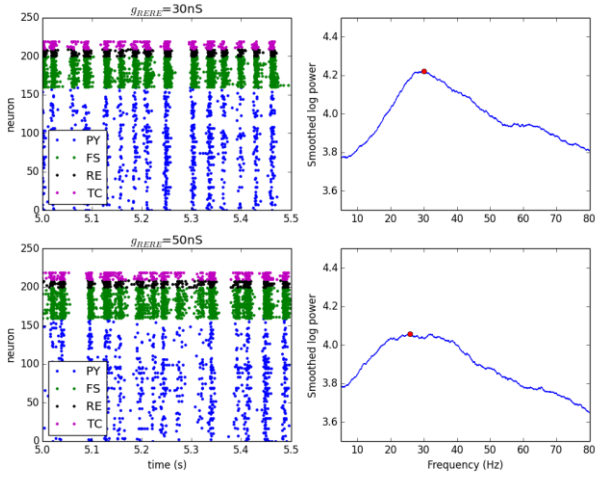

Figure 3. (Left) Raster plots indicate spike times of cortical and thalamic cells for the cases in which the synaptic conductance between RE cells is 30nS (top) and 50nS (bottom). (Right) Smoothed power spectrum of simulated EEG signals generated as described in the models and methods section. An increase in synaptic conductance from 30nS (top) to 50nS (bottom) leads to a decrease and broadening in the oscillatory frequency.

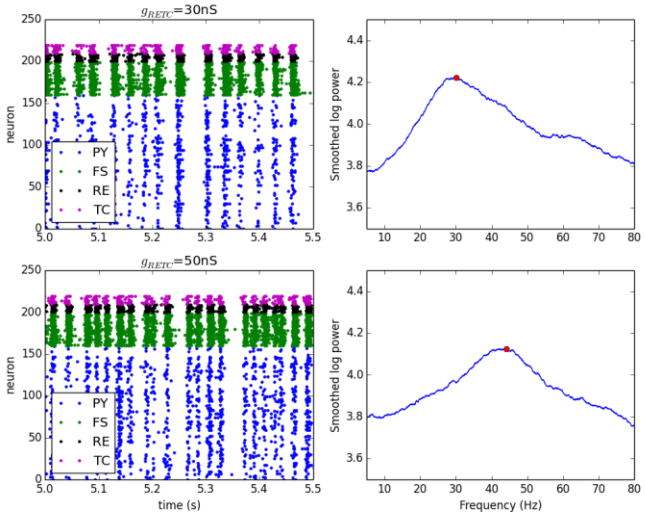

Figure 4. (Left) Raster plots indicate spike times of cortical and thalamic cells for the cases in which the synaptic conductance from RE to TC cells is 30nS (top) and 50nS (bottom). (Right) Smoothed power spectrum of simulated EEG signals show an increase in synaptic conductance from 30nS (top) to 50nS (bottom) leads to a faster oscillation.

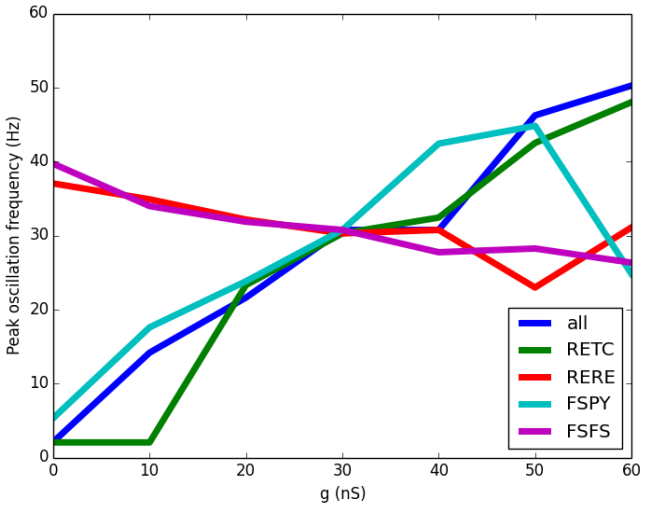

Figure 5. Network oscillatory frequency as a function of synaptic conductance. An increase in inhibitory synaptic conductance onto excitatory neurons (FS-PY and RE-TC) was correlated with an increase in oscillation frequency, and the opposite trend was true for the inhibitory synaptic conductance onto inhibitory neurons (FS-FS and RE-RE). In the case in which all inhibitory synaptic current strengths in the circuit were modified simultaneously, oscillatory frequency increased.

3.3 Inhibitory synaptic time constant effect on oscillatory frequency

Similarly to how an increase in synaptic conductance yields a stronger IPSP, a decrease in the synaptic time constant yields a broader IPSP, also resulting in more current flow out of the cell. The summation of IPSPs from multiple inhibitory presynaptic cells would elicit a more negative hyperpolarization if their time constants were increased. Therefore, we hypothesized that in addition to a synapse's conductance, its decay dynamics would also modulate the frequency at which the network oscillated. In the experiment performed, the

time constant of inhibitory synapses was varied between 7.5ms and 20ms in increments of 2.5ms. However, modifying the time constant had no regular effect on the rhythm of the network, as shown in Figure 6.

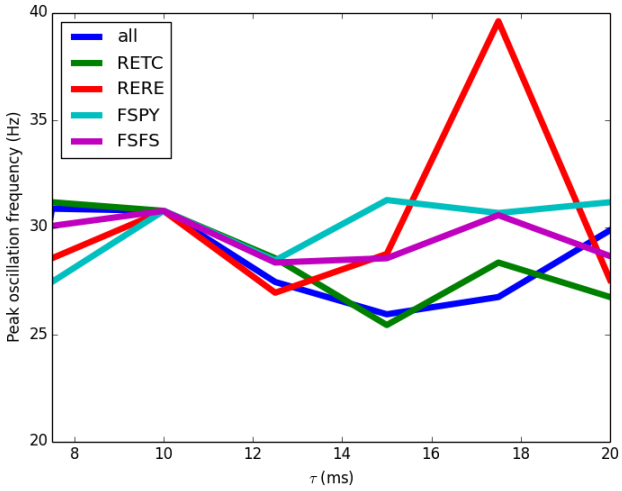

Figure 6. Network oscillatory frequency as a function of synaptic time constant. No consistent effect was observed either by shortening or elongating the synaptic decay time for a single class of inhibitory projections or all inhibitory projections.

3.4 Network dynamics state transition

Using the Izhikevich model, we aimed to replicate the same findings as those in sections 3.2 & 3.3. However, we report here an interesting phenomenon when a large increase (24µS to 144µS) in inhibitory synaptic conductance is applied to reticular-relay (RETC) synapses. Figure 7a. shows the simulated EEG trace (400ms) for both low (top) and high (bottom) conductance conditions. Both EEG recordings are periodic and have similar frequencies (~13Hz), however, visual inspection of the traces informs us that the two conditions are under drastically different behavioral states, which the spike raster plots (Figure 7b.) confirm. In the low conductance condition, all neurons are consistently firing, and the EEG periodicity comes from weakly synchronized quiescent windows in the pyramidal population. In the high conductance condition, the network has sharply divided UP and DOWN states, where all firing stop completely during the DOWN state. The thalamic neurons initiate the UP state, leading the population firing and triggering an avalanche of spikes in the cortical population. The latter behavior are similar to previously described burst firing of thalamic cells during sleep.

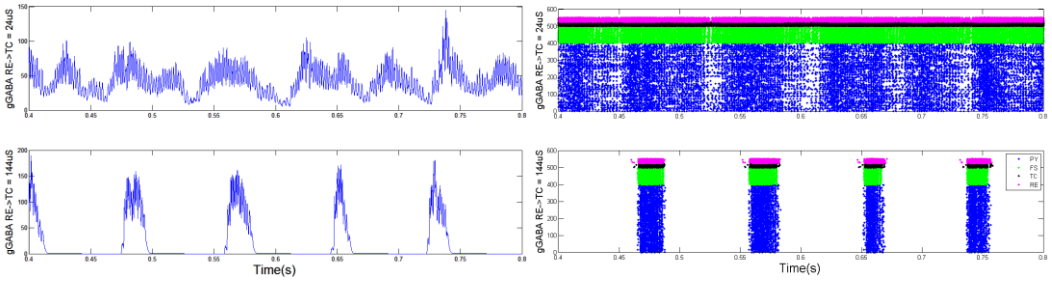

Figure 7. a) (left) Estimated EEG recording for 400ms. Top: g_{GABA} = 24µS, bottom: 144µS. b) (right) Spike raster plot of all neurons, blue: PY, green: FS, black: TC, pink: RE

To investigate the cause of the state change, we focus on the firing dynamics of one particular

thalamocortical relay cell (Figure 8a.), which has excitatory connections to all other neuron groups. In the low conductance condition, the relay cells fire consistently and rapidly throughout the simulation, whereas they display a much slower recovery from hyperpolarization after the previous UP state in the high conductance condition. This behavior is consistent with most accounts of the thalamic relay cell, where two distinct modes of firing – tonic and phasic – are observed due to activation of slow calcium dynamics [10]. A closer look at the phase diagram reveals the underlying neural dynamics (Figure 8b.): when inhibitory conductance between reticular and relay cells is low, the range of recovery variable (u) is small, and the entire dynamics resides in the high-u portion of the space. This is likely due to an upward shift of the node/limit cycle as inhibitory currents have little effects in canceling out the excitatory currents. In comparison, high inhibitory conductance causes a downward shift of the limit cycle, effectively equalizing the excitatory input and enables the slower dynamics.

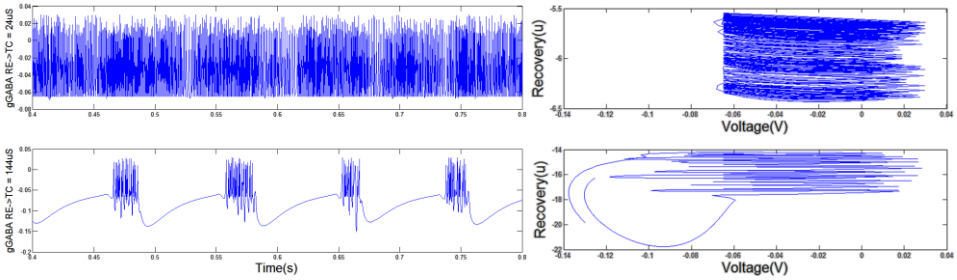

Figure 8. a) (left) Simulated voltage trace of one thalamocortical relay (TC) cell. Top: g_{GABA} = 24µS, bottom: 144µS. b) (right) Phase diagram of the same TC cell in a), plotting voltage against Izhikevich recovery variable, u

Finally, to demonstrate that this qualitative change in behavior is not only an epiphenomenon, but has functional significance in the cortical network, pairwise firing correlation between pyramidal cells are computed (Figure 9). Under tonic firing of the relay cells, pyramidal cell activity remains largely uncorrelated, save for small clusters of neurons, though never exceeding a correlation coefficient of 0.5 (mean = 0.11). Under phasic (or burst) firing, however, pyramidal neuron activity becomes highly correlated (mean = 0.63). Correlated firing encourages information preservation during transfer due to increased redundancy, but decreases total information rate, which is consistent with the observation that information processing is turned down during sleep or other states of unconsciousness, such as one induced through propofol inhalation.

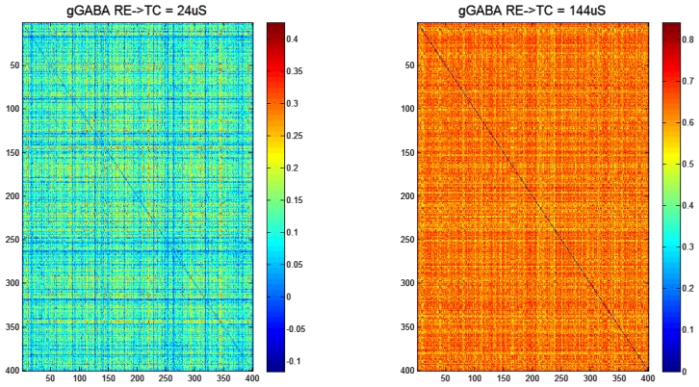

Figure 9. Spike correlation of all pyramidal neurons. Left: g_{GABA} = 24µS, mean pairwise correlation = 0.11; right: 144µS, mean = 0.63

4 Conclusion

To summarize, we simulate the effect of altering GABAergic current conductance and decay time in specific inhibitory synapses has on macroscopic oscillation frequency using aeIF and Izhikevich neurons. We present three main findings using a previously established thalamocortical model. First, oscillation frequency changes due to increased inhibitory conductance are dependent on post-synaptic neuron type: faster oscillations if the post-synaptic neuron is excitatory, and slower if inhibitory. When all inhibitory synaptic conductances are increased in concert, network oscillation frequency increases, likely driven by the large number of pyramidal cells in the model. Second, changes in inhibitory current decay time have no effect on oscillation frequency, at least in the biologically plausible regime we explored. Third, large changes in inhibitory conductance can produce dynamic changes in the network behavior that is uncaptured by peak oscillation frequency, switching from regular spiking of all neurons to periodic ON-OFF states driven by thalamocortical cells.

Our findings have important implications for studying macroscopic oscillations, as well as using specific oscillatory bands as clinical marker. Since altering synaptic conductance in different synapses have different effects on the overall oscillation, GABA-enhancing drugs (e.g. propofol) may act differently depending on the particular receptors of a post-synaptic cell. Although we only demonstrate the effect of this specificity on macroscopic oscillations, it likely has cognitive consequences as well. In addition, EEG rhythm has long been used as a measure of anesthetic levels. As such, our results suggest that a closer examination of oscillatory dynamics should be considered in the context of different synaptic pairings, especially when unexpected phenomenon occurs, such as propofol-induced paradoxical excitation [11].

Finally, we propose several extensions of our work. First, a natural continuation is to consider the effects of altering excitatory synaptic parameters on network oscillation, as well as other network parameters such as connection probability, synaptic delays, and model parameters for both aeIF and Izhikevich neurons. Second, since macroscopic oscillations have been implicated in synchronization of neuron spiking, our model can be extended by feeding back the estimated local field into individual neurons. Lastly, behavioral studies should be conducted to experimentally validate the computational findings, in order to fine-tune the model such that it can be used in meaningful applications.

Acknowledgments

The authors thank instructor Dr. Gert Cauwenberghs and teaching assistants Jonathan Garcia, Chul Kim, and Bruno Pedroni for their help throughout the course and project. Dr. ShiNung Ching of Washington University in St. Louis provided some reference code for a similar thalamocortical model and also suggestions for other resources.

References

[1] Buzsáki, G., & Draguhn, A. (2004). Neuronal oscillations in cortical networks. *Science* **304**(5679): 1926-1929.

[2] Başar, E., Başar-Eroğlu, C., Karakaş, S., & Schürmann, M. (1999). Are cognitive processes manifested in event-related gamma, alpha, theta and delta oscillations in the EEG?. *Neuroscience letters* **259**(3): 165-168.

[3] Lopes da Silva, F. (1991). Neural mechanisms underlying brain waves: from neural membranes to networks. *Electroencephalography and clinical neurophysiology* **79**(2): 81-93.

[4] Destexhe, A., & Sejnowski, T. J. (2003). Interactions between membrane conductances underlying thalamocortical slow-wave oscillations. *Physiological reviews* **83**(4): 1401-1453.

[5] Nunez PL, Srinivasan R. (2005) *Electric Fields of the Brain: The Neurophysics of EEG*. New York, NY: Oxford Univ Press.

[6] Ching, S., Cimenser, A., Purdon, P. L., Brown, E. N., & Kopell, N. J. (2010). Thalamocortical model for a propofol-induced α-rhythm associated with loss of consciousness. *Proceedings of the National Academy of Sciences* **107**(52): 22665-22670.

[7] Goodman, D. F., & Brette, R. (2009). The Brian Simulator. *Frontiers in neuroscience* **3**(2): 192.

[8] Destexhe, A. (2009). Self-sustained asynchronous irregular states and Up-Down states in thalamic, cortical, and thalamocortical networks of nonlinear integrate-and-fire neurons. *Journal of Computational Neuroscience* **27**(3): 493-506

[9] Brette, R., & Gerstner, W. (2005). Adaptive exponential integrate-and-fire model as an effective description of neuronal activity. *Journal of neurophysiology* **94**(5): 3637-3642.
[10] Izhikevich, E. M. (2003). Simple model of spiking neurons. *IEEE Transactions on neural networks* **14**(6): 1569-1572.
[11] McCarthy M. M, Brown, E. N, Kopell, N. (2008) Potential network mechanisms mediating electroencephalographic beta rhythm changes during propofol-induced paradoxical excitation. J Neurosci. 10;28(50):13488-504. doi: 10.1523/JNEUROSCI.3536-08.2008